

# 1 A chronology of alluvial fan response to Late Quaternary sea level 2 and climate change, Crete

3 Richard J.J. Pope <sup>a,\*</sup>, Ian Candy <sup>b</sup>, Emmanuel Skourtsos <sup>c</sup>

4  
5 <sup>a</sup> Geography and Earth Systems Science, University of Derby, Kedleston Road, Derby, DE22 1GB, UK

6 <sup>b</sup> Department of Geography, Royal Holloway, University of London, Egham, Surrey, TW20 0EX, UK

7 <sup>c</sup> Department of Dynamic, Tectonic and Applied Geology, Faculty of Geology and Geoenvironment, National  
8 & Kapodistrian University of Athens, Panepistimioupolis Zografou, 15784, Greece

## 10 **Introduction**

11 The Mediterranean basin lies at the climatic boundary between arid North Africa and  
12 temperate mid-latitude Europe (Harding et al., 2009; Tzedakis, 2009; Rohling et al., 2015)  
13 and is, consequently, highly sensitive to environmental change. This sensitivity is well-  
14 expressed in the palaeo-record (Allen et al., 1999; Moreno et al., 2004). Marine and  
15 speleothem records from the Mediterranean provide clear evidence for temperature and  
16 rainfall variations on both orbital and millennial/centennial timescales during the Late  
17 Quaternary (Cacho et al., 1999; 2000; Emeis et al., 2003; Bar-Matthews et al., 1999; 2003).  
18 Many researchers have subsequently suggested that these archives record climatic events that  
19 are the correlatives of the high-magnitude/high-frequency Dansgaard-Oeschger events that  
20 are preserved in the Greenland ice core record (Bar-Matthews et al., 1999; 2003; Sánchez  
21 Goñi, et al., 2002; Moreno et al., 2004). The long pollen records that are preserved in the  
22 sedimentary basins of this region show that ecosystems of the Mediterranean are also highly  
23 sensitive to environmental fluctuations and provide evidence for vegetation response on both  
24 orbital and sub-orbital timescales (Allen et al., 1999; Tzedakis, et al., 2003).

25 As prevailing climate and vegetation will dictate surface hydrology and sediment supply,  
26 there is good reason to suppose that surface processes, such as fluvial systems, should also be  
27 highly responsive to Late Quaternary environmental dynamics (Rose and Meng, 1999; Rose  
28 et al., 1999; Macklin et al., 2002; 2012). This suggestion has been supported by a number of  
29 pioneering studies that have applied a range of geochronological techniques (primarily  
30 luminescence-based approaches and U-series techniques) to fluvial sediments and landforms  
31 from a number of catchments across the Mediterranean basin (see Fuller et al., 1998; Rose  
32 and Meng, 1999; Rose et al., 1999; Rowan et al., 2000; Candy et al., 2004; 2005; Pope and  
33 Wilkinson, 2005; Pope et al., 2008; Adamson et al., 2014). These studies suggest a broad  
34 consistency in Mediterranean fluvial response with phases of large-scale alluviation  
35 correlating to cold-dry stadial environments, i.e. Marine Isotope Stages (MIS) 5d, 4 and 2,

36 whilst warm-moist interstadial/interglacial environments, i.e. MIS 5e and 5a, appear to be  
37 characterised by either widespread catchment stability or by fluvial incision (Rose et al.,  
38 1999; Macklin et al., 2002). A number of authors have also proposed that sediment/landform-  
39 evidence for fluvial response to abrupt climatic events during MIS 3 can be observed in  
40 several Mediterranean catchments (Fuller et al., 1998; Macklin et al., 2012). Such studies are  
41 part of a consistent palaeoenvironmental narrative that highlights the sensitivity of  
42 Mediterranean environments, ecologies and geomorphic systems to climate forcing.

43 The early attempts to construct chronologies for Mediterranean fluvial archives have a  
44 number of limitations that restrict a full understanding of the relationship between climate  
45 forcing and geomorphic response. These limitations are primarily related to the dating  
46 techniques that have been applied and can be placed into two categories: 1) the magnitude of  
47 uncertainties associated with the ages and with the resulting age estimates for fluvial  
48 response, and 2) the number of age estimates that are used to constrain a fluvial sequence. For  
49 example, OSL ages of Mallorcan alluvial fan sequences by Rose and Meng (1999) and Rose  
50 et al. (1999) defines a phase of alluviation to MIS 5d (age estimate = 109.2 ka) but the  
51 uncertainties associated with that age are twice the duration of the substage with which the  
52 alluviation phase is correlated (uncertainties =  $\pm 16.7$  ka). Furthermore, many of these  
53 chronologies are based on a relatively small number of age estimates. For example, U-series  
54 dating of river terraces of the Rio Aguas in southeast Spain has been used to produce a  
55 landform chronology for the past 300 ka but this is based on just 13 dates (Candy et al., 2004;  
56 2005). Furthermore, the Sparta basin chronology of Pope and Wilkinson (2005) is  
57 constrained by just 14 OSL ages, spread across multiple fan systems and spanning the last  
58 240 ka. Consequently, although the timing of fluvial response in some of these studies  
59 appears to relate to climate forcing it could be argued that such conclusions are based on a  
60 restricted number of age estimates and a more extensive dataset is required to robustly prove  
61 such a relationship.

62 It should be highlighted that these comments are not a criticism of these studies, but a  
63 reflection of the limitation of the techniques that existed at the time that such work was  
64 undertaken. A number of developments in both OSL and U-series dating over the past 20  
65 years has meant that it is now possible to routinely analyse samples that were previously  
66 problematic for dating and to generate age estimates of much greater precision (Murray and  
67 Wintle, 2000; 2003; 2006; van Calsteren and Thomas, 2006; Geach et al., 2015). It is now

68 possible to produce more extensive fluvial chronologies with lower uncertainties, allowing  
69 better links between geomorphic response and climate forcing.

70 In this study we present an OSL and U-series based chronology for the small (surface area =  
71 <6.5 km<sup>2</sup>) Sphakia alluvial fan, in southwest Crete. This alluvial fan has been described  
72 elsewhere (Nemec and Postma, 1993; 1995; Pope et al., 2008; Ferrier and Pope, 2012). On  
73 the basis of detailed mapping and U-series dating, the formation of Sphakia fan has  
74 previously been placed within a Quaternary timeframe and comprises three main phases of  
75 alluviation (segments 1, 2 and 3) separated by downcutting and fan entrenchment (Nemec  
76 and Postma, 1993; 1995). The new chronology presented here is based on >30 age estimates.  
77 The dataset is used to: 1) test the agreement between the OSL and U-series age estimates in  
78 order to assess the validity of the derived chronology; 2) test whether the main phases of fan  
79 entrenchment are associated with significant changes in either sea level or climate; and 3)  
80 determine if there is a clear link between the timing of fan alluviation and cold/dry stadial  
81 climates. The paper discusses the factors that drive alluviation and incision within Sphakia  
82 fan over the late Quaternary and concludes by highlighting the importance of generating  
83 extensive chronological datasets to robustly understand the timing of Quaternary fluvial  
84 response.

## 85 **Regional setting and site context**

86 The Sphakia fan is one of a number of alluvial fans along the Sphakian piedmont in  
87 southwestern Crete (Pope et al., 2008; Figure 1). The Sphakian piedmont forms a prominent  
88 24-km long and 1.5 to 2.5-km wide east to west trending coastal plain between Chora  
89 Sphakia and Skaloti (Figure 1). The piedmont represents the onshore segment of the southern  
90 Cretan margin and preserves a complex regional sedimentary history relating to the interplay  
91 of tectonics and climate over Late Neogene to Quaternary timescales (Skourtsos et al., 2007).  
92 Following the formation of the extensive Sphakian fault system, the piedmont underwent  
93 rapid subsidence culminating in the deposition of Miocene to lower Pleistocene littoral sands,  
94 marls, and clays (Skourtsos et al., 2007). Subsequent uplift and the gradual re-emergence of  
95 the piedmont at the end of the lower Pleistocene led to significant erosion of marine  
96 sediments and formation of a low relief sub-aerial platform that provided the accommodation  
97 space for coalescent alluvial fans (Skourtsos et al., 2007).

98 The southern margin of the east-west piedmont is clearly marked by a 10 to 30 m high coastal  
99 cliff that formed by a combination of marine erosion and continued tectonic activity during

100 the Holocene (Postma and Nemeč, 1990). The northern margin of the piedmont is delimited  
101 by the southeastern flanks of the Lefka Ori range (Pope et al., 2008). Structurally, the Lefka  
102 Ori is the southernmost portion of a late Eocene to early Oligocene thrust-pile, comprising  
103 intensely folded carbonates, meta-siliclastic sediments, mica-schists and quartzites of late  
104 Triassic to late Cretaceous age (Skourtsos et al., 2007). Continuous uplift since the late  
105 Pliocene has elevated the Lefka Ori to create four distinctive zones (Pope et al., 2008): 1). the  
106 high mountains (c.2400 to 1700 m amsl) comprising karstic landscapes thought to have been  
107 sculpted by glaciers associated with a localised Pleistocene ice cap; 2). the lower  
108 glacial/periglacial mountainous zone (c.1700 to 900 m amsl) that serves as the main sediment  
109 source area for the piedmont; 3). the foothills (900 to 200 m amsl); and 4). the badaja (<200  
110 m amsl), which comprises nine coalescing fans dissected by a series of north-south trending  
111 gorges.

112 Intermittent alpine savanna comprising *Cupressus sempervirens* and *Juniperus oxycedrus*  
113 extends across the high mountain zone and defines the tree line at c.1500 m amsl (Rackham  
114 and Moody, 1996). Below the savanna, extensive woodland dominated by *Pinus brutia* and  
115 *Quercus coccifera* occupies a well-defined altitudinal zone (200 to 1300 m amsl) across the  
116 lower mountain and foothill zones, with phrygana and steppe covering the coastal plain  
117 (Nixon et al. 1988). The region is characterised by a highly seasonal precipitation regime  
118 with rainfall concentrated into the late autumn and winter period. Mean annual rainfall is  
119 estimated to range between c.180 mm on the coastal plain (Nemeč and Postma, 1993) and  
120 800 to 1100 mm in the mountain zone (Rackham and Moody, 1996). For the high mountain  
121 zone estimated annual rainfall varies between 1500 and 2000 mm, producing significant  
122 snow cover during between the winter and late spring period (Rackham and Moody, 1996).

123 The Sphakia fan (Figure 1) occupies the western end of the piedmont (Nemeč and Postma,  
124 1993; Pope et al., 2008; Ferrier and Pope, 2012). This fan is fed by a steep-sided and  
125 entrenched gorge, which drains zones 1 to 3 of the Lefka Ori. The three telescopic segments  
126 occur downstream of the entrenched fan headcut (Figure 2). These segments comprise three  
127 main phases of fan aggradation (Pope et al., 2008); segment 1 (oldest), segment 2 and  
128 segment 3 (the youngest). Field surveys confirm that segment 2 consists of three distinct  
129 surfaces namely 2A (oldest), 2B and 2C (youngest [Figure 3]). Each segment consists of  
130 aggradations of sediment that are primarily coarse-grained (cobble and pebble dominated  
131 with occasional boulders) with interbedded, laterally discontinuous units of fine to medium  
132 sands and silts (Nemeč and Postma, 1993; Pope et al., 2008). Two types of coarse-grained

133 deposit can be identified (Figure 4); 1) poorly-sorted units with a high proportion of fine  
134 (silt/clay) matrix (typically matrix supported) or 2) moderately-sorted units of sands and  
135 gravels (typically clast-supported fabric). These sediment types are suggested to reflect the  
136 operation of mass-flow/debris-flow (poorly-sorted, matrix-supported sediments) and  
137 current/fluvial flow (moderately-sorted, clast supported sediments) (Pope et al., 2008).  
138 Deposits of segment 2 and 3 are dominated by the moderately-sorted/clast supported  
139 sediments suggesting that, during these episodes of fan aggradation, fluvial sedimentation  
140 was the dominant process (Pope et al., 2008). Deposits of segment 1 contain both poorly-  
141 sorted/matrix-supported sediments and moderately-sorted/clast supported sediments,  
142 implying that both fluvial and debris flow processes played a significant role during this  
143 phase of fan aggradation (Pope et al., 2008). The segment 1 and 2 deposits have undergone  
144 localised cementation by secondary carbonate. These cements predominantly consist of large,  
145 equant spar crystals that are typical of phreatic cements (Candy et al., 2012).

## 146 **Methodology**

### 147 *Optically Stimulated Luminescence (OSL) ages*

148 Twenty four samples from Sphakia fan were collected in copper tubes (5 cm in diameter and  
149 20 cm in length) from sections logged by Pope et al. (2008). Potentially light exposed  
150 material from the tube ends was removed and used to for measuring *in-situ* water content.  
151 The quartz fraction of the 180–250  $\mu\text{m}$  size was obtained by sieving, 10% HCl and H<sub>2</sub>O<sub>2</sub>  
152 treatments, heavy liquid density separation, and 20% HF etching (Murray et al., 1987). All  
153 quartz particles were screened for contamination by feldspars by examining the response to  
154 infrared stimulated luminescence (IRSL) with contaminated samples undergoing further HF  
155 treatments and infrared bleaching. Following these treatments, approximately 300 grains  
156 were mounted on 9.8 mm diameter stainless-steel discs prior to measurement. All  
157 luminescence measurements were carried out in accordance with the single-aliquot  
158 regenerative (SAR) protocol of Murray and Wintle (2000, 2003). The equivalent dose (De)  
159 for each quartz-rich extract was calculated from radionuclide concentrations and cosmic ray  
160 contributions based upon each sample's burial depth (Prescott and Hutton, 1994). To assess  
161 the reliability of the measured SAR data all samples were subjected to dose recycling and  
162 dose recovery tests using a 10-s preheat range of 240-260°C. Age estimates were derived by  
163 dividing De by the total dose rate (D).

164

165 *U-series dating*

166 Eight carbonate samples were collected using a hammer and chisel. Wherever possible,  
167 carbonates were sampled in close proximity and in stratigraphic relationship to OSL samples  
168 so that ages derived by the two methods could be directly compared. In almost all cases  
169 phreatic spar cements were targeted as these, like speleothems, are well-suited for U-series  
170 dating (van Calsteren and Thomas, 2006), being; 1) densely-cemented and consequently  
171 resistant to post-formational U/Th loss or gain, and 2) relatively pure with minimal detrital  
172 contamination. Samples that contained  $^{230}\text{Th}/^{232}\text{Th}$  ratios of  $<20$  were considered to be  
173 detritally contaminated (Cr-015, Cr-019 and Cr-025). These samples were corrected using an  
174 assumed detrital ratio following the procedure of Clark-Balzan et al. (2012). The other  
175 samples contained  $^{230}\text{Th}/^{232}\text{Th}$  ratios from 20 up to 418, although detrital corrections will  
176 change the ages of these sediments, the corrected ages are still within the uncertainty of the  
177 original age and so corrections were not carried out.

178 In the laboratory, thin sections of each sample were investigated by optical microscopy for  
179 evidence of recrystallisation, porosity, and multiple growth layers. Where multiple layers  
180 occurred, samples were extracted from particular crystal layers using a low-powered  
181 microscope. U-series sample preparation, separation geochemistry and mass spectrometry  
182 techniques follow the procedure of Seth et al. (2003). The U/Th isotopic ratios of the  
183 carbonate samples were analysed by an IsoProbe multicollector ICP-MS at Royal Holloway  
184 University of London (see Seth et al., 2003 for details and operating parameters), using static  
185 mode on Faraday collectors and the ion-counting Daly detector in the axial position. U and  
186 Th analyses were carried out for a mass range 228 to 238. Th and U were analysed  
187 separately, with mass  $^{230}\text{Th}$  and  $^{234}\text{U}$  on the Daly detector used to measure Th and U isotope  
188 ratios samples were run in conjunction with total procedural blanks and rock standards (Table  
189 Mountain Latite and the OU Young speleothem).

190 **Results**

191 The morphology and sedimentology of Sphakia fan has been discussed in Pope et al. (2008)  
192 and Ferrier and Pope (2012), consequently only the dating results are discussed here. The  
193 OSL and U-series analytical data are shown, along with the derived age estimates, in Tables 1  
194 and 2. Dates are shown against the stratigraphic profiles in Figure 5. The dates are described  
195 in the following section by fan segment.

196

197 *Chronology of fan segment 1*

198 Fan sediments relating to segment 1 were analysed at sections A, B and C. The nine OSL  
199 ages, four from section A, four from section B, and one from section C, span a range between  
200  $144 \pm 15$  ka and  $72 \pm 3$  ka and are in stratigraphic order (Figure 5 and Table 1). Two U-series  
201 ages from section A yield ages of  $123.9 \pm 7.4$  ka and  $75.4 \pm 2.9$  ka, whilst one age of  $70.9 \pm 1.0$   
202 ka was generated from section B (Figure 5 and Table 2).

203 *Chronology of fan segment 2*

204 Sediments of segment 2A are poorly exposed. Section D represents the most extensive record  
205 of this phase of fan aggradation however, the absence of fine-grained units and the strong  
206 degree of cementation in this section made it unsuitable for OSL dating. Two U-series ages  
207 were derived from this section (Figure 5), one from a phreatic cement towards the base of the  
208 sequence ( $72.3 \pm 6.1$  ka) and one from a carbonate clast rind at the land surface associated  
209 with a weakly developed pedogenic calcrete ( $59.0 \pm 2.3$  ka). These, two samples have  
210  $^{230}\text{Th}/^{232}\text{Th}$  ratios of  $<7$  and were, therefore, corrected following the procedure outlined  
211 above. The dates quoted here are the corrected ages.

212 Section E records a sediment profile through segment 2B sediments. In this section carbonate  
213 cementation was either absent or the cements were too porous to be appropriate for U-series  
214 dating. Three OSL ages were derived from this section. From the lower gravel units upwards  
215 these ages are:  $55 \pm 4$ ,  $49 \pm 4$  and  $28 \pm 2$  ka (Figure 5).

216 Sections F and G record sediments of segment 2C. Section F is a coastal exposure within one  
217 of the thickest parts of the fan sequence and has yielded seven OSL ages which are all in  
218 stratigraphic agreement. From the base upwards these ages are:  $102 \pm 10$ ,  $71 \pm 4$ ,  $46 \pm 5$ ,  $40 \pm 3$ ,  
219  $20 \pm 2$ ,  $14.2 \pm 1.5$  and  $11.2 \pm 0.7$  ka. Two U-series ages have been derived from phreatic  
220 cements below the oldest OSL age ( $102 \pm 10$  ka) and yield ages of  $300 \pm 21$  ka and  $172.8 \pm 4.3$   
221 ka, respectively. A third U-series age of  $>350$  ka has been derived from a reworked flow  
222 stone from the lowest (currently) exposed gravel unit. The lowermost 2 to 3 metres of  
223 sediments are suggested to represent an older sedimentary unit which is separated from the  
224 overlying deposits by a hiatus or erosional unconformity. This is proposed because; 1) there  
225 is a significant time gap between the ages of the lowermost 2 to 3 metres and those of the  
226 overlying deposits, and 2) the degree of diagenesis and the pattern of sediment alteration in  
227 the lowermost 2 to 3 metres is different from that in the overlying sediments. The lowermost  
228 sediments are very heavily indurated and contain complex faults and fractures, infilled with

229 phreatic carbonates up to 15 cm thick, that are entirely absent in the overlying sediments. The  
230 deposits exposed in section G have yielded five OSL ages, again in good stratigraphic  
231 agreement. From the base of the section upwards, these ages are:  $18.2 \pm 1.2$ ,  $17.2 \pm 1.2$ ,  $16.1$   
232  $\pm 1.1$ ,  $15.2 \pm 1.1$  and  $13.8 \pm 1.2$  ka.

### 233 *Chronology of fan segment 3*

234 There were limited exposures through segment 3 sediments and, where sediments were  
235 available, they contain insufficient fine-grained sediment for OSL dating and no visible  
236 carbonate cements. This unit was not, consequently, dated. Nevertheless, a later prehistorical  
237 age (2500 to 1000 BC) for the fine-grained segment 3 sediments is provided by well-  
238 preserved Middle to Late Minoan sherds exposed within in the distal part of Patsianos fan  
239 (Sphakia survey, 2002; see also Figure 1 of Pope et al., 2008).

## 240 **Interpretation of the Sphakia fan chronology and system response**

### 241 *Reliability of the OSL and U-series chronology*

242 The reliability of the derived age estimates can be assessed in the following ways. Firstly,  
243 through the stratigraphic integrity observed within the OSL ages in each section. In each  
244 sequence the ages become progressively younger upward without age inversions. Secondly,  
245 the consistency of the derived ages with the relative ages of the individual fan sediments e.g.  
246 ages from segment 2 deposits are younger than those derived from segment 1 deposits. The  
247 youngest OSL age ( $72 \pm 3$  ka) from the top of section A and the OSL age ( $71 \pm 4$ ka) from  
248 segment 2 sediments are coeval but there are no ages from segment 1 deposits that are  
249 demonstrably younger than those from segment 2 deposits. Furthermore, this implies that the  
250 incisional phase that occurred between segments 1 and 2 was relatively short.

251 The chronologies for the fan segments 2A, 2B and 2C, are more complicated. In general  
252 terms the ages from these units are in stratigraphic agreement. The U-series age from the  
253 pedogenic carbonate that caps the surface of the segment 2A deposits in section D is  $59.0$   
254  $\pm 2.3$  ka, implying that accretion of this unit had ceased prior to this date. The oldest age  
255 within segment 2B deposits (section E) is  $55 \pm 4$  ka and is, therefore, stratigraphically  
256 consistent with the U-series age for the end of segment 2A accretion. There is, however,  
257 overlap between the OSL ages of segments 2B and those of segment 2C. The youngest age  
258 derived from segment 2B is  $28 \pm 2$  ka and the oldest ages in the segment 2C sediments are  $46$   
259  $\pm 5$  ka and  $40 \pm 3$  ka (Figure 5; Table 1). This implies that sedimentation was still occurring on



260 the segment 2B surface whilst segment 2C sediments were beginning to accumulate. This  
261 scenario is not impossible. In the mid- and lower-fan areas of the Sphakia system the  
262 difference between the height of the 2B and 2C surfaces is minimal i.e. typically less than  
263 2m. Furthermore, the fan surface is fed by a series of tributary systems that drain directly  
264 onto the surface of the fan. It is possible that sedimentation was coeval in part on the surfaces  
265 of segment 2B and 2C.

266 The OSL and U-series age estimates are consistent and this suggests that the chronology is  
267 robust (See Clark-Balzan et al., 2012). However, OSL ages date the age of sediment  
268 deposition and burial. In contrast U-series ages date the age of carbonate cementation of the  
269 host sediments; consequently they post-date deposition. As a result, for the same sampling  
270 location, the OSL ages should always be older than the U-series ages.

271 This is the pattern observed throughout the Sphakia sequences wherever OSL and U-series  
272 ages are paired (e.g. in section A, approximately 10 metres above the section base, the OSL  
273 age is  $84 \pm 8$  ka and the U-series age of the carbonate that cements this sediment is  $75.4 \pm 2.9$   
274 ka. Such consistency also exists in section B; an OSL age of  $81 \pm 4$  ka at 9 metres above the  
275 base is associated with a cementation age of  $70.9 \pm 1.0$  ka. In section F a sand unit with an  
276 OSL age of  $102 \pm 10$  ka is underlain by a gravel unit whose carbonate cement dates to  $172.8$   
277  $\pm 4.3$  ka. A lower gravel unit is cemented by carbonate that dates to  $300 \pm 21$  ka, while the  
278 lowest (currently exposed) gravels contain reworked flow stone that dates to  $>350$  ka. As  
279 these different ages are consistent and the stratigraphic order of the ages is maintained  
280 throughout all the sequences the derived chronology can be used to discuss the timing of  
281 different phases of alluviation within the Sphakia system.

### 282 *Relationship between the timing of geomorphic response within the Sphakia system to Late* 283 *Quaternary environmental change*

284 The timing of geomorphic response within the Sphakia alluvial fan is placed into  
285 environmental context in two ways. First, the age-range covered of each fan segment (i.e.  
286 segment 1, 2A, 2B and 2C) and the timing of fan entrenchment can be compared to local and  
287 regional records of environmental change (Figure 6). Second, OSL ages for alluviation can be  
288 separated from their stratigraphic context and plotted against the local and regional records of  
289 environmental change to establish whether patterns or clusters of ages occur and whether or  
290 not these relate to specific climatic intervals (Figure 7). There are no long records of  
291 palaeoenvironmental change from Crete that span the time interval represented by the

292 Sphakia chronology. A  $U^{k'}_{37}$  (unsaturated ratio of long-chain ketones) derived sea surface  
293 temperature (SST) record has been constructed from marine core M40-4/71 that was  
294 collected southwest of the Sphakian piedmont (Emesis et al., 2003 and see Figure 1). Key  
295 regional records from the eastern Mediterranean are also used; the long-pollen record of  
296 Tenaghi Philippon (Tzedakis et al., 2001; 2004) and the  $\delta^{18}O$  speleothem record from Soreq  
297 cave (Bar-Matthews et al., 1999; 2003). Both of these records should be strongly controlled  
298 by precipitation regime/aridity but may also contain a temperature component. These three  
299 palaeoenvironmental archives can be compared to the stacked benthic  $\delta^{18}O$  record of Lisiecki  
300 and Raymo (2005).

301 The ages from segment 1 span the final part of MIS 6 and the whole of MIS 5 with the  
302 youngest age from this unit ( $72 \pm 3$  ka) corresponding to the early part of MIS 4 (Figure 5).  
303 Fan entrenchment occurs after this but alluviation resumed by late MIS 4. This is consistent  
304 with the U-series ages for the carbonate cements that have formed within the sediments of  
305 section D which implies that, at this site, segment 2 alluviation had begun by ca 72ka.  
306 Incision and fan entrenchment must, therefore, have occurred during MIS 4. The OSL ages  
307 derived from segment 2 sediments span MIS 3, MIS 2 and early MIS 1. The top 3 metres of  
308 sections F and G date to the late MIS 2 and MIS 1 and correspond to the Lateglacial interval.  
309 The youngest OSL age within the segment 2 deposits is  $11.2 \pm 0.7$  ka, implying that the  
310 incision and entrenchment between segment 2 and 3, and the deposition of the segment 3  
311 sediments themselves, must have occurred after this date i.e. during the Holocene (Figure 6).

312 The literature on investigating links between alluvial fan process and climate forcing, on both  
313 long and short term timescales, is extensive (see Bull, 1979; Ritter et al., 1995; McDonald et  
314 al., 2002; Bacon et al., 2010; Miller et al., 2010). In this study we place our results primarily  
315 in the context of the Mediterranean literature on fluvial response to Quaternary climate  
316 change as this is the region of most relevance to the present study. The response of the  
317 Sphakia fan, as outlined above, can be linked to environmental forcing through the concept of  
318 critical power (Bull, 1979, see also Mather et al., 2000). That is to say that under conditions  
319 where stream power, primarily a function of discharge and channel gradient, exceeds  
320 resistance power, primarily a function of sediment load and calibre, critical power, the power  
321 needed to transport all available sediment, is overcome and the fluvial system will begin to  
322 incise and the alluvial fan will become entrenched (Bull, 1979). Conversely, under conditions  
323 where the stream power is lower than the resistance power, the threshold of critical power is  
324 not exceeded and the fluvial system is incapable of transporting all of the sediment available

325 from the catchment (Bull, 1979). Under these conditions the fan will undergo alluviation or  
326 aggradation. These ideas are closely linked to environmental change (Rose and Meng, 1999;  
327 Rose et al., 1999). For example climate, through its impact on vegetation density/type and  
328 patterns/rates of weathering, will control the nature and rate of sediment supply (Rose et al.,  
329 1999; Macklin et al., 2002; Candy et al., 2004; 2005). Furthermore, long term changes in  
330 precipitation regime, through the magnitude and frequency of rainfall events, will strongly  
331 control the discharge and stream power of the system (Harvey and Wells, 1987). Finally, sea  
332 level changes coupled with the steep near-shore gradients associated with the southern Cretan  
333 margin will control the magnitude of channel gradient across the fan system (Alves et al.,  
334 2007; Waters et al., 2010). Major falls in sea level will greatly increase channel gradient  
335 which will potentially increase stream power sufficiently to trigger fluvial incision and  
336 entrenchment (Waters et al., 2010). The ages associated with the two key phases of fan  
337 entrenchment in the Sphakia system, segment 1 to 2 and segment 2 to 3, suggest that incision  
338 occurred in association with two of the key climatic transitions of the last 125,000 years; 1)  
339 the major cooling and rapid lowering of sea level that occurred between MIS 5a and 4, and 2)  
340 the climatic amelioration that occurred during the transition into the current interglacial.

341 It is during the MIS5a/4 transition that the greatest decrease in global sea levels occurred  
342 (Waelbroeck et al., 2002; Siddall et al., 2003). This transition does not represent the glacial  
343 maximum or the lowest sea level during the last glacial (Waelbroeck et al., 2002). However,  
344 during the MIS 5a/4 transition sea levels fell by 70 to 100 metres over ca 10,000 yrs  
345 (Waelbroeck et al., 2002; Siddall et al., 2003). It is proposed here that this sea level fall  
346 associated with the steep offshore gradients of the southern Cretan margin caused an increase  
347 in the channel gradient across the Sphakia fan surface. The transition into MIS 4 was,  
348 therefore, characterised by fan entrenchment. It is noticeable that the other major fall in sea  
349 level during the last glacial (the MIS 3/2 transition) has no clear response in alluvial fan  
350 dynamics. In relative terms, the fall in sea level between MIS 3 and 2 was smaller than in  
351 MIS 5a/4 (Waelbroeck et al., 2002; Siddall et al., 2003) resulting in less of an effect on the  
352 fan. However, it is also important to note that the ages associated with segment 2 alluviation  
353 imply that entrenchment between segments 2A/2B and 2B/2C occurred during MIS 3 and 2.  
354 It is, therefore, possible that part of the geomorphic complexity associated with the segment 2  
355 fan surface could reflect base level changes during this interval. The overlap between ages in  
356 some of these deposits indicates that attributing an absolute timescale to these geomorphic  
357 shifts is not currently possible.

358 The shift from fan aggradation during MIS 2 to incision during the Holocene, which is  
359 represented in the Sphakia fan by entrenchment after the accumulation of segment 2 deposits  
360 but prior to the deposition of segment 3 deposits, is a phenomena that is seen in many  
361 catchments across the Mediterranean (White et al., 1996; Rose et al., 1999; Rowan et al.,  
362 2000; Macklin et al., 2002; Candy et al., 2004; 2005; Pope and Wilkinson, 2005). This is  
363 widely suggested to be a response to climatic controlled changes in hydrology and sediment  
364 supply rather than gradient shifts associated with sea level change. During stadials, such as  
365 during MIS 2, palaeoclimatic and palaeoecological records indicate that, in the  
366 Mediterranean, climates were arid (Bar-Matthews et al., 1999; 2003), vegetation was  
367 dominated by *Artemisia* steppe (Pons and Reille, 1988; Allen et al., 1999; Tzedakis et al.,  
368 2003; Margari et al., 2009) and weathering rates were high (Rose et al., 1999). These  
369 conditions resulted in high rates of sediment supply to catchments producing river systems  
370 that did not have sufficient stream power to transport this load and consequently they  
371 underwent aggradation/alluviation. At the onset of the Holocene, the increase in moisture  
372 availability resulted in an increase in vegetation cover and a recolonization of the landscape  
373 by woodland (Pons and Reille, 1988; Allen et al., 1999; Tzedakis et al., 2003; Margari et al.,  
374 2009), this stabilisation of the landscape reduced sediment supply which, in combination with  
375 wetter climates, overcame the threshold of critical power causing incision (Candy et al.,  
376 2004). This model is also the most likely explanation for the episode of fan entrenchment  
377 between segments 3 and 2.

378 Despite climate being proposed as the cause of fan entrenchment between fan segments 2 and  
379 3 the currently accepted model of fluvial response to Quaternary climate change in the  
380 Mediterranean, i.e. aggradation during stadials and incision/stability during interglacials and  
381 interstadials (Macklin et al., 2002), is not seen in the Sphakia chronology. That is to say that  
382 although many of the OSL ages do constrain alluviation phases to stadial climates, alluviation  
383 is not restricted to such intervals. The OSL chronology for Sphakian sedimentation phases  
384 shows no clear relationship to any particular climatic type or MIS with alluvial sediments  
385 dating to (see Figure 6): interglacials (ages from segment 1 deposits of  $123.9 \pm 7.4$  ka and  $124$   
386  $\pm 10$  ka correspond to MIS 5e), interstadials (ages from the segment 1 deposits of  $84 \pm 8$  ka  
387 and  $81 \pm 4$  ka date to MIS 5a), stadials within MIS 5 (with OSL ages of  $101 \pm 8$  ka and  $102$   
388  $\pm 10$  ka corresponding to MIS 5d), interstadials from the last glacial (ages from segment 2  
389 deposits of  $55 \pm 4$  ka,  $48 \pm 4$  ka and  $46 \pm 5$  ka correspond to the main climatic peak of MIS 3)  
390 and stadials from the coldest parts of the last glacial (ages from segment 2 deposits of  $20 \pm 2$ ka

391 and  $18.2 \pm 1.2$  ka correspond to the climatic minima of MIS 2). Clearly between each of the  
392 dated levels in these sequences there are sediments that have no age associated age estimates,  
393 consequently, the OSL chronology presented here is not a definitive record of the timing of  
394 alluviation within the Sphakian sequence. However, the dates presented do not show a clear  
395 relationship between alluviation and any specific climatic types. This is in contrast with other  
396 such studies from the Mediterranean that show a clustering of alluviation phases around  
397 glacial/stadial climates (Rose and Meng, 1999; Rose et al., 1999; Rowan et al., 2000;  
398 Macklin et al., 2002; 2012; Candy et al., 2004 and 2005; Pope and Wilkinson, 2005). The  
399 dataset presented here, therefore, suggests that alluviation in the Sphakia system was a  
400 persistent process that operated across the entire last interglacial/glacial cycle (Figure 7).

#### 401 **Discussion**

402 The chronology generated from sediments sequences of the Sphakia fan is different from  
403 previous summaries of Quaternary fluvial activity in the Mediterranean. In this fan there is no  
404 clear relationship between the age of alluviation and orbital scale climate change of the Late  
405 Quaternary. The established chronology implies that, with the exception of the two fan  
406 phases of entrenchment, rates of sediment supply to the Sphakia fan during most of the last  
407 interglacial/glacial cycle were sufficient to cause the fan to aggrade rather than incise. The  
408 climate and vegetation of the Mediterranean, during stadials, produced landscapes that were  
409 highly susceptible to erosion and, consequently, the sediment yield was high. Alluviation  
410 within the Sphakia fan during interglacials and interstadials is more surprising as the  
411 extensive and higher density vegetation cover of such intervals is supposed to produce more  
412 stable landscape that would generate lower sediment yield (e.g. Pope and Wilkinson, 2005).

413 To place the Sphakia chronology into context it is useful to compare this record with that of  
414 Rose and Meng (1999) and Rose et al. (1999) from alluvial fans on Mallorca. In the  
415 Mallorcan sequences climatic ameliorations (MIS 5e, 5c and 5a) are characterised by fan  
416 surface stability and pedogenesis and fan alluviation is restricted to stadial climates (MIS 5d,  
417 5b, 4 and 2). The Mallorcan fan sequences, therefore, show a clear response to Quaternary  
418 climate change and one which is consistent with our understanding of the control played by  
419 climate (partly through vegetation) on hydrology and sediment supply. In the Mallorcan  
420 sequences sediment supply to fan systems appears to be greatly reduced, or even switched off  
421 during interglacials and interstadials, whereas in the Sphakia fan, even during interglacials,  
422 the supply of sediment was capable of causing alluviation and preventing fan surface

423 stabilisation or entrenchment. It is here suggested that the most probable cause for the  
424 difference in fan response between these two study regions is catchment topography.

425 The Mallorcan fan systems drain relatively low hills (maximum altitude ca 560 metres amsl  
426 (Rose et al., 1999)), whereas the Sphakia fan drains high mountainous region reaching up to  
427 2452 metres amsl (Pope et al., 2008). The relatively low altitude of the Mallorcan hills means  
428 that for most of the Late Quaternary they were rarely characterised by cold mountain climate.  
429 When this moderate climate is combined with the rainfall of ca 500 mm/a, they are always  
430 likely to be well-vegetated and, therefore, limited in sediment supply. Only during the  
431 extremes of climatic deteriorations i.e. the stadial episodes of the last interglacial/glacial  
432 cycle, are temperatures and rainfall likely to decrease enough to cause vegetation to decline  
433 to expose areas of bare-ground and allow sediment supply to increase. It is, therefore,  
434 postulated that, in such a subdued topography, drastic climatic deteriorations are required to  
435 trigger fan alluviation (see Rose et al., 1999).

436 The Sphakia fan operates in a different topographic setting, draining high mountains with  
437 present-day tree line around 900 metres below the highest peaks (Rackham and Moody,  
438 1996). This produces large areas of exposed bedrock which, combined with the high rainfall  
439 (up to 1100 mm/a), means that the fan source areas have the potential to both generate and  
440 transport sediment even during the interglacial conditions of the present day. Consequently,  
441 major climatic deteriorations are not required to stimulate fan alluviation and this system has  
442 the potential to undergo alluviation during both interglacials, interstadials and stadials.

443 The ages of alluvial fan sedimentation presented above are different from that proposed by  
444 Macklin et al. (2002; 2012) which argued for a consistent pan-Mediterranean response of  
445 fluvial systems to Quaternary climate change. Although it could be argued that this difference  
446 is a function of the specific conditions in the catchment of the Sphakia fan it is important to  
447 highlight that several of the studies presented in the Macklin et al. (2002) compilation are  
448 also high altitude catchments. They are, therefore, also sensitive to the same factors that  
449 would have affected alluvial fan aggradation in southern Crete. Consequently, it is not simply  
450 the case that the topographic setting of the Sphakia fan makes it insensitive to climate forcing  
451 in comparison to other fluvial systems that have previously been studied. Fundamentally, it is  
452 important to recognise that the twenty four OSL dates and eight U-series ages make the  
453 Sphakia system the most dated small alluvial system in the Mediterranean constraining the  
454 timing of fluvial response more strongly than any previously published record. Furthermore,

455 the uncertainties associated with each age (average uncertainty of ca 9%), are lower than the  
456 uncertainties associated with the ages presented in Macklin et al. (2002), which are typically  
457  $\geq 10\%$  of the derived age. This reflects the development of chronological techniques over the  
458 last 15 years. The dataset presented here, therefore, advances the discussion of fan response  
459 to climate change because not only are there sufficient ages to allow the timing of fan  
460 alluviation to be discussed, but also the age estimates are of high enough precision to allow  
461 them to be robustly correlated with specific marine isotopic stages and substages. Whether  
462 the idea of a consistent pattern of Quaternary fluvial response across the Mediterranean is  
463 valid or whether catchment specific factors play a key role in the timing of alluviation can  
464 only be truly understood with detailed studies in the style of that presented here. If the role of  
465 long-term forcing on Quaternary geomorphic response in the Mediterranean is to be  
466 understood in detail this can only be achieved by the production of sediment/landform  
467 chronologies that are based on large numbers of high-precision age estimates.

## 468 **Conclusions**

469 A coupled OSL and U-series chronology has been constructed for the Sphakia alluvial fan in  
470 southern Crete. This chronology is based on 32 age estimates showing that the evolution of  
471 this fan spanned the time interval from late MIS 6 through to the Holocene. The  
472 entrenchment that occurs between the different stages of fan aggradation corresponds to MIS  
473 4 (the incision that occurs between fan segments 1 and 2) and the early Holocene (the  
474 incision that occurs between fan segments 2 and 3). The incision that generates this  
475 entrenchment is suggested to be a function of sea level fall, which drives the incision between  
476 fan segments 1 and 2, and the climatic amelioration at the onset of the Holocene, which  
477 appears to drive the incision between fan segments 2 and 3. In contrast the timing of fan  
478 alluviation shows no correlation to any specific climatic state with dated fan sediments  
479 corresponding to interglacial, interstadial and stadial episodes. This is in strong contrast to the  
480 majority of Quaternary fluvial studies in the Mediterranean which correlate alluviation phases  
481 to stadial events. It is likely that the topographic setting of the Sphakia fan, a steep catchment  
482 which drains a high mountain region much of which is currently above the treeline, means  
483 that sediment supply during most climatic stages of the Late Quaternary is sufficient to  
484 promote persistent alluviation across the Late Quaternary. Despite these catchment specific  
485 conditions it is also suggested that the large number of ages presented here, and their  
486 relatively high-precision, allows the timing of fan alluviation to be understood in more detail  
487 in the Sphakia system than in any other currently dated Mediterranean geomorphic sequence.

488 Only through the application of large numbers of high-precision age estimates can the timing  
489 of alluviation in Quaternary fluvial sequences be robustly constrained and such an approach  
490 is necessary to test whether the previously proposed synchronicity in the response of  
491 Mediterranean river systems to Quaternary environmental change is truly valid.

## 492 **Acknowledgements**

493  
494 The authors would like thank Adrian Harvey and the anonymous reviewer for their very  
495 constructive comments and suggestions, which has greatly improved the structure of the  
496 paper. We also acknowledge the British Society of Geomorphology for providing funding to  
497 support the fieldwork. Additionally, Pope acknowledges funding from the Royal Geographic  
498 Society to cover the costs of the U-series dating. The OSL dating was undertaken at the Risø  
499 National Luminescence laboratory. Permission to undertake the fieldwork in Crete was  
500 granted by the Institute for Geological and Mineral Exploration.

## 501 **References**

502

503 Adamson, K. R., Woodward, J. C., Hughes, P. D., 2014. Glaciers and rivers: Pleistocene uncoupling  
504 in a Mediterranean mountain karst. *Quaternary Science Reviews*, 94, 28-43.

505 Allen, J.R.M., Brandt, U., Brauer, A., Hans-Wolfgang, H., Huntley, B., Keller, J., Krami, M.,  
506 Mackensen, A., Mingram, J., Negendank, J.F.W., Nowaczyk, N.R., Oberhansli, H., Watts, W.A.,  
507 Wulfg, S., Zolitschka, B., 1999. Rapid environmental changes in southern Europe during the last  
508 glacial period, *Nature*, 400, 740–743

509 Alves, T. M., Lykousis, V., Sakellariou, D., Stamatina, A., Nomikou, P., 2007. Constraining the origin  
510 and evolution of confined turbidite systems: southern Cretan margin, Eastern Mediterranean Sea  
511 (34°30–36°N) *Geo-Marine Letters*, 27, 1, 41-61.

512

513 Bacon, S.N., McDonald, E.V., Caldwell, T.G., Dalldorf, G.K., 2010. Timing and distribution of  
514 alluvial fan sedimentation in response to strengthening of late Holocene ENSO variability in the  
515 Sonoran Desert, southwestern Arizona, USA. *Quaternary Research* 73, 425-438.

516

517 Bar-Matthews, M., Ayalon, A., Kaufman, A., Wasserburg, G. J., 1999. The Eastern Mediterranean  
518 palaeoclimate as a reflection of regional events: Soreq, Israel. *Earth and Planetary Science Letters*,  
519 166, 85-95.

520 Bar-Matthews, M., Ayalon, A., Gilmour, M., Matthews, A., Hawkesworth, C. J., 2003. Sea-land  
521 oxygen isotopic relationships from planktonic foraminifera and speleothems in the Eastern  
522 Mediterranean region and their implications for palaeorainfall during interglacial intervals.  
523 *Geochimica et Cosmochimica Acta*, 67, 3181-3199

524 Bull, W.B., 1979. Threshold of critical power in streams. *Geological Society of America Bulletin*. 90,  
525 453-464.

526 Cacho, I., Grimalt, J.O., Pelejero, C., Canals, M., Sierro, F.J., Flores, J.A. Shackleton, N.J., 1999.  
527 Dansgaard-Oeschger and Heinrich event imprints in Alboran Sea palaeotemperatures.  
528 *Palaeoceanography*, 14, 698-705

529

530 Cacho, I., Grimalt, J.O., Sierro, F.J., Shackleton, N., Canals, M., 2000. Evidence for enhanced  
531 Mediterranean thermohaline circulation during rapid climatic coolings. *Earth and Planetary Science*  
532 *Letters*, 183, 417-429



533 Candy, I., Black, S., Sellwood, B.W., 2004. Interpreting the response of a dryland river system to Late  
534 Quaternary climate change. *Quaternary Science Reviews*, 23, 2513-2523

535 Candy, I., Black, S., Sellwood, B.W., 2005. U-series isochron dating of immature and mature  
536 calcretes as a basis for constructing Quaternary landform chronologies for the Sorbas basin, southeast  
537 Spain. *Quaternary Research*, 64, 100-111.

538 Candy, I., Adamson, K., Gallant, C.E., Whitfield, E., Pope, R., 2012, Oxygen and carbon isotopic  
539 composition of Quaternary meteoric carbonates from western and southern Europe: Their role in  
540 palaeoenvironmental reconstruction. *Palaeogeography, Palaeoclimatology, Palaeoecology*, 326–328, 1-  
541 11.

542 Clark-Balzan, L.A., Candy, I., Schwenninger, J.L., Bouzouggar, A., Blockley, S.P., Nathan, R.,  
543 Barton, N., 2012. Coupled U-series and OSL dating of a Late Pleistocene cave sediment sequence,  
544 Morocco, North Africa: Significance for constructing Palaeolithic chronologies. *Quaternary*  
545 *Geochronology*, 12, 53-64.

546 Emeis, K.-C., Schulz, H., Struck, U., Rossignol-Strick, M., Erlenkeuser, H., Howell, M. W., Kroon,  
547 D., Mackensen, A., Ishizuka, S., Oba, T., Sakamoto, T., Koizumi, I., 2003. Eastern Mediterranean  
548 surface water temperatures and  $\delta^{18}\text{O}$  composition during deposition of sapropels in the late  
549 Quaternary, *Paleoceanography*, 18, 1005, 1-18.

550 Ferrier, G. and Pope, R.J.J., 2013. Quantitative mapping of alluvial fan evolution using ground-based  
551 reflectance spectroscopy. *Geomorphology*, 175-176, 14-24.

552 Fuller, I.C., Macklin, M.G., Lewin, J., Passmore, D.G., Wintle, A.G., 1998. River response to high  
553 frequency climate oscillations in southern Europe over the past 200ky. *Geology*, 26, 3, 275-278.

554 Geach, M.R., Thomsen, K.J., Buylaert, J.-P., Murray, A.S., Mather, A.E., Telfer, M.W., Stokes, M.,  
555 2015. Single-grain and multi-grain OSL dating of river terrace sediments in the Tabernas Basin, SE  
556 Spain. *Quaternary Geochronology*, 30, Part B, 213–218.

557 Harding, A.E., Palutikof, J., Holt, T., 2009, *The Climate System*. In: Woodward, J.C. (Ed), *The*  
558 *Physical Geography of the Mediterranean*, Oxford University Press, Oxford, 69-88

559 Harvey, A.M., Wells, S.G., 1987. Response of Quaternary fluvial systems to differential epeirogenic  
560 uplift: Aguas and Feos river systems, southeast Spain. *Geology*, 15, 689-693.

561 Harvey, A.M., 2002. The role of base-level change in the dissection of alluvial fans: case studies from  
562 southeast Spain and Nevada. *Geomorphology*, 45, 67-87.

563 Harvey, A.M., Silva, P.G., Mather, A.E., Goy, J.L., Stokes, M., Zazo, C., 1999. The impact of  
564 Quaternary sea-level and climatic change on coastal alluvial fans in the Cabo de Gata range, southeast  
565 Spain. *Geomorphology*, 28, 1-22.

566 Lisiecki, L.E., Raymo, M.E., 2005. A Pliocene-Pleistocene stack of 57 globally-distributed  
567 benthic  $\delta^{18}\text{O}$  records. *Paleoceanography* 20, PA1003.

568 Ludwig, K.R., 2003. *ISOPLLOT 3.00*. United States Geological Survey.

569 Macklin, M.G., Fuller, I.C., Lewin, J., Maas, G.S., Passmore, D.G., Rose, J., Woodward, J.C., Black,  
570 S., Hamlin, R.H.B., Rowan, J.S., 2002. Correlation of fluvial sequences in the Mediterranean basin  
571 over the last 200 ka and their relationship to climate change. *Quaternary Science Reviews*, 21, 1633-  
572 1641.

573  
574 Macklin, M.G., Lewin, J., Woodward, J.C., 2012. The fluvial record of climate change. *Philosophical*  
575 *Transactions of the Royal Society A*, 370, 2143-2172.

576

577 Margari, V., Gibbard, P.L., Bryant, C.L., Tzedakis, P.C., 2009. Character of vegetational and  
578 environmental changes in southern Europe during the last glacial period; evidence from Lesvos  
579 Island, Greece. *Quaternary Science Reviews* 28, 13/14, 1317–1339.  
580

581 Mather, A.E., Harvey, A.M, Stokes, M., 2000. Quantifying long-term catchment changes of alluvial  
582 fan systems. *Geological Society of America Bulletin*, 112, 1825-1833.  
583

584 McDonald, E.V., McFadden, L.D., Wells, S.G., 2002. Regional response of alluvial fans to the  
585 Pleistocene-Holocene climatic transition, Mojave Desert, California. In: Enzel, Y., Wells, S.G.,  
586 Lancaster, N. (Eds.), *Paleoenvironments and Paleohydrology of the Mojave and Southern Great Basin*  
587 *Deserts*. Geological Society of America, Boulder, Colorado.  
588

589 Miller, D.M., Schmidt, K.M., Mahan, S.A., McGeehin, J.P., Owen, L.A., Barron, J.A., Lehmkuhl, F.,  
590 Lehrer, R., 2010. Holocene landscape response to seasonality of storms in the Mojave Desert.  
591 *Quaternary International* 215, 45-61.  
592

593 Moreno, A., Cacho, I., Canals, M., Grimalt, J.O., Vidal, A.S., 2004. Millennial-scale variability in the  
594 productivity signal from the Alboran Sea record, Western Mediterranean Sea. *Palaeogeography,*  
595 *Palaeoclimatology, Palaeoecology*, 211, 205-219.  
596

597 Murray, A.S., Wintle, A.G., 2000. Luminescence dating of quartz using an improved single-aliquot  
598 regenerative-dose protocol. *Radiation Measurements* 32, 1, 57–73.  
599

600 Murray, A.S., Wintle, A.G., 2003. The single aliquot regenerative-dose protocol: potential for  
601 improvements in reliability. *Radiation Measurements*, 37, 377-381.  
602

603 Murray, A.S., Wintle, A.G., 2006. A review of quartz optically stimulated luminescence  
604 characteristics and their relevance in single-aliquot regeneration dating protocols. *Radiation*  
605 *Measurements*, 41, 369-391.

606 Murray, A.S., Marten, R., Johnston, A. Martin, P., 1987 Analysis for naturally occurring  
607 radionuclides at environmental concentrations by gamma spectrometry. *Journal of Radioanalytical*  
608 *and Nuclear Chemistry*, 115, 2, 263-288.

609 Nemec, W., Postma, G., 1993. Quaternary alluvial fans in southwestern Crete: sedimentation  
610 processes and geomorphic evolution. In: Marzo, M., Puigdefábregas, C. (Eds), *Alluvial*  
611 *Sedimentation*. Special Publication of the International Association of Sedimentologists, 17, 235-276.

612 Nemec, W., Postma, G., 1995. Quaternary alluvial fans in southwestern Crete: sedimentation  
613 processes and geomorphic evolution: A reply. *Sedimentology*, 42, 535-549.  
614

615 Nixon, L., Moody, J., Rackham, O., 2000. Archaeological survey in Sphakia, Crete. *Echos du Monde*  
616 *Classique*, XXXII, 7, 159-173.  
617

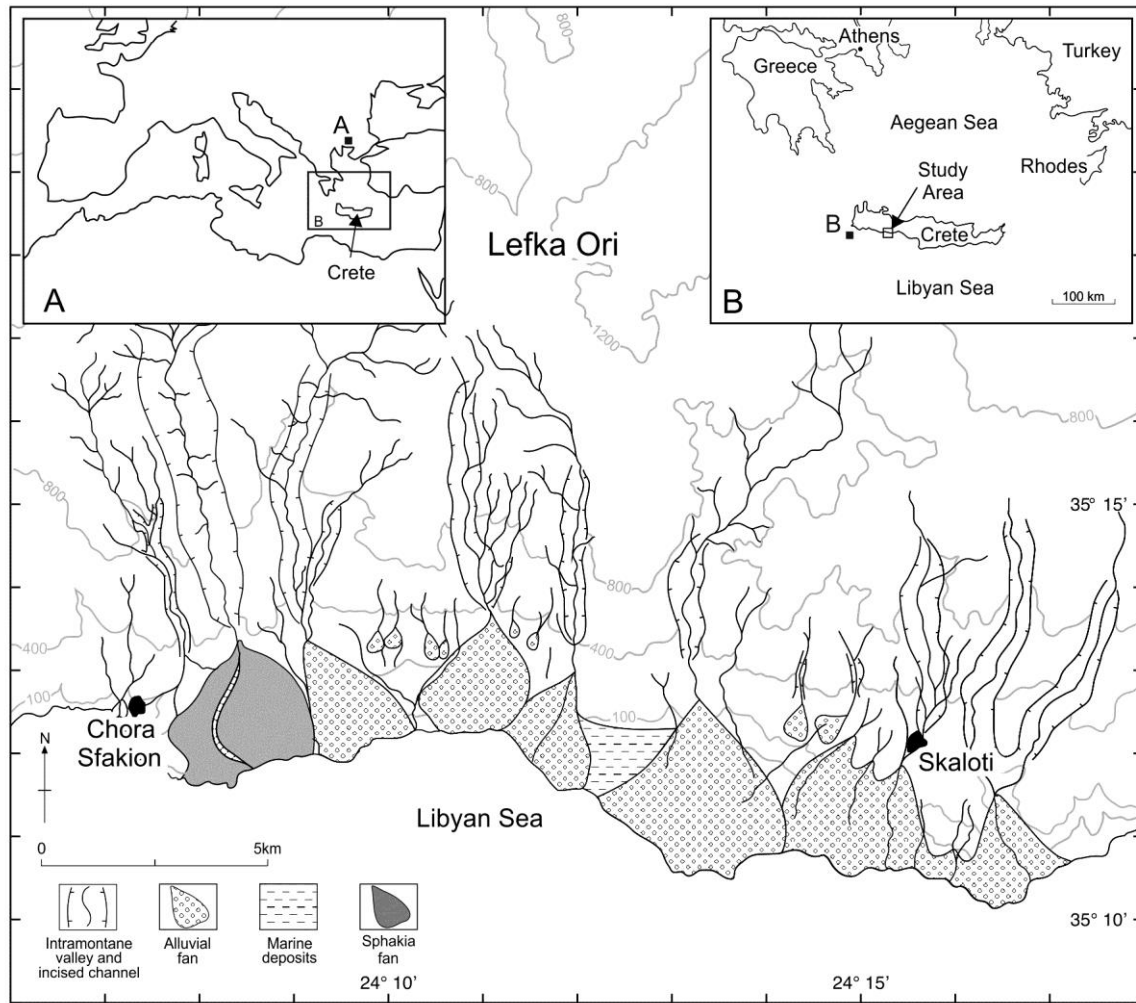
618 Pons, A., Reille, M., 1988. The Holocene- and upper Pleistocene pollen record from Padul (Granada,  
619 Spain): A new study. *Palaeogeography, Palaeoclimatology, Palaeoecology*, 66, 243-263.

620 Pope, R. J. J., Wilkinson, K.N., 2005. Reconciling the roles of climate and tectonics in Late  
621 Quaternary fan development on the Spartan piedmont, Greece. In: Harvey, A.M., Mather, A.E.,  
622 Stokes, M. (Eds.), *Alluvial fans: Geomorphology, Sedimentology, Dynamics*. Geological Society  
623 *Special Publication*, 251, 133-152.  
624

- 625 Pope, R. J.J., Wilkinson, K.N., Skourtsos, E., Triantaphyllou, M., Ferrier, G., 2008. Clarifying stages  
626 of alluvial fan evolution along the Sfakion piedmont, southern Crete: new evidence from soil  
627 magnetism and OSL dating. *Geomorphology* 94, 206–225.
- 628 Postma, G. & Nemeč, W. (1990) Regressive and transgressive sequences in a raised Holocene  
629 gravelly beach, southwestern Crete. *Sedimentology*, 37, 907-920.
- 630 Prescott, J.R., Hutton, J.T. (1994) Cosmic ray contributions to dose rates for luminescence and ESR  
631 dating: Large depths and long-term time variations. *Radiation Measurements*, 23, 2–3, 497–500
- 632 Rackham, O., Moody, J., 1996. *The making of the Cretan landscape*. Manchester University Press,  
633 Manchester.
- 634 Ritter, J.B., Miller, J.R., Enzel, Y., Wells, S.G., 1995. Reconciling the roles of tectonism and climate  
635 in Quaternary alluvial fan formation. *Geology* 23, 245-248.  
636
- 637 Rohling, E.J., Marino, G., Grant, K.M., 2015. Mediterranean climate and oceanography and the  
638 periodic development of anoxic events (sapropels). *Earth-Science Reviews*, 143, 62-97.
- 639 Rose, J., Meng, X.M., 1999. River activity in small catchments over the last 140 ka, northeast  
640 Mallorca, Spain. In: Brown, A.G. and Quine., T. (Eds), *Fluvial processes and environmental change*.  
641 Wiley and sons, Chichester, 91-102.
- 642 Rose, J., Meng, X.M., Watson, C., 1999. Palaeoclimate and palaeoenvironmental responses in the  
643 western Mediterranean over the last 140ka; evidence from Mallorca, Spain. *Journal of the Geological*  
644 *Society*, London, 156, 435-448.
- 645 Rowan, J.S., Black, S., Macklin, M.G., Tabner, B.J., Dore, J., 2000. Quaternary environmental change  
646 in Cyrenaica evidenced by U-Th, ESR and OSL of coastal alluvial fan sequences. *Libyan Studies*, 31,  
647 5–16.
- 648 Sánchez Goñi, M. F. Cacho, I., Turon, J.-L., Guiot, J., Sierro, F.J., Peyrouquet, J.-P., Grimalt, J. O.,  
649 Shackleton, N. J. 2002. Synchronicity between marine and terrestrial responses to millennial scale  
650 climatic variability during the last glacial period in the Mediterranean region. *Climate Dynamics*, 19,  
651 95–105.
- 652 Seth, B., Thirlwall, M.F., Houghton, S.L., Craig, C.A., 2003. Accurate measurements of Th-U isotope  
653 ratios for carbonate geochronology using MC-ICP-MS. *Journal of Analytical Atomic Spectrometry*,  
654 18, 1323-1330.
- 655 Shackleton, N.J., Imbrie, J., Hall, M.A. 1983. Oxygen and carbon isotope record of East Pacific core  
656 V19-30: implications for the formation of deep water in the late Pleistocene North Atlantic. *Earth and*  
657 *Planetary Science Letters*, 65, 233–244.
- 658 Siddall, M., Rohling, E. J., Almogi-Labin, A., Hemleben, Ch., Meischner, D., Schmelzer, I., Smeed,  
659 D.A., 2003. Sealevel fluctuations during the last glacial cycle. *Nature*, 423, 853-  
660 858.  
661
- 662 Skourtsos, E., Pope, R.J.J., Triantaphyllou, M., 2007. Tectono-sedimentary evolution and rates of  
663 tectonic uplift of the Sphakia coastal zone, southwest Crete. *Bulletin of the Geological Society of*  
664 *Greece*, XXXVII, 475-487
- 665 Sphakia Survey, 2002. *The Sphakia Survey: Internet Edition*. (<http://sphakia.classics.ox.ac.uk/>  
666 [accessed 22 May 2016]).
- 667 Stokes, M., Mather, A.E. 2000. Response of Plio-Pleistocene alluvial systems to tectonically induced  
668 base-level changes, Vera Basin, SE Spain. *Journal of the Geological Society*, London, 157, 303-316.

- 669 van Calsteren, P. Thomas, L., 2006. Uranium-series dating applications in natural environmental  
670 science. *Earth Science Reviews*, 75, 1-4, 155–175.
- 671 Tzedakis, P.C. Andrieu, V., de Beaulieu, J.-L., Birks, H.J.B., Crowhurst, S., Follieri, M.,  
672 Hooghiemstra, H., Magri, D., Reille, M., Sadori, L., Shackleton, N.J., Wijmstra, T.A., 2001.  
673 Establishing a terrestrial chronological framework as a basis for biostratigraphical comparisons.  
674 *Quaternary Science Reviews* 20, 1583-1592.
- 675 Tzedakis, P.C., McManus, J.F., Hooghiemstra, H., Oppo, D.W., Wijmstra, T.A., 2003. Comparison of  
676 changes in vegetation in northeast Greece with records of climate variability on orbital and suborbital  
677 frequencies over the last 450,000 years. *Earth and Planetary Science Letters*, 212, 197-212.
- 678 Tzedakis, P.C., Frogley, M.R., Lawson, I.T., Preece, R.C., Cacho, I., de Abreu, L., 2004. Ecological  
679 thresholds and patterns of millennial-scale climate variability: The response of vegetation in Greece  
680 during the last glacial period. *Geology*, 32, 2, 109-112.
- 681 Tzedakis, P.C., 2009, *Cenozoic Climate and Vegetation Change*. In: Woodward, J.C. (Ed.), *The*  
682 *Physical Geography of the Mediterranean*, Oxford University Press, Oxford, 89-137.
- 683 Waelbroeck, C., Labeyrie, L., Michel, E., Duplessy, J.C., McManus, J.F., Lambeck, K., Balbon, E.,  
684 Labracherie, M., 2002. Sea-level and deep water temperature changes derived from benthic  
685 foraminifera isotopic records. *Quaternary Science Reviews* 21, 295-305
- 686 Waters, J.V., Jones, S.J. Armstrong, H.A., 2010. Climatic controls on late Pleistocene alluvial fans,  
687 Cyprus *Geomorphology*, 115, 3–4, 228–251
- 688 White, K., Drake, N., Millington, A., Stokes, S., 1996. Constraining the timing of alluvial fan  
689 response to Late Quaternary climatic changes, southern Tunisia. *Geomorphology* 17, 295–304
- 690

691 **List of Figures**

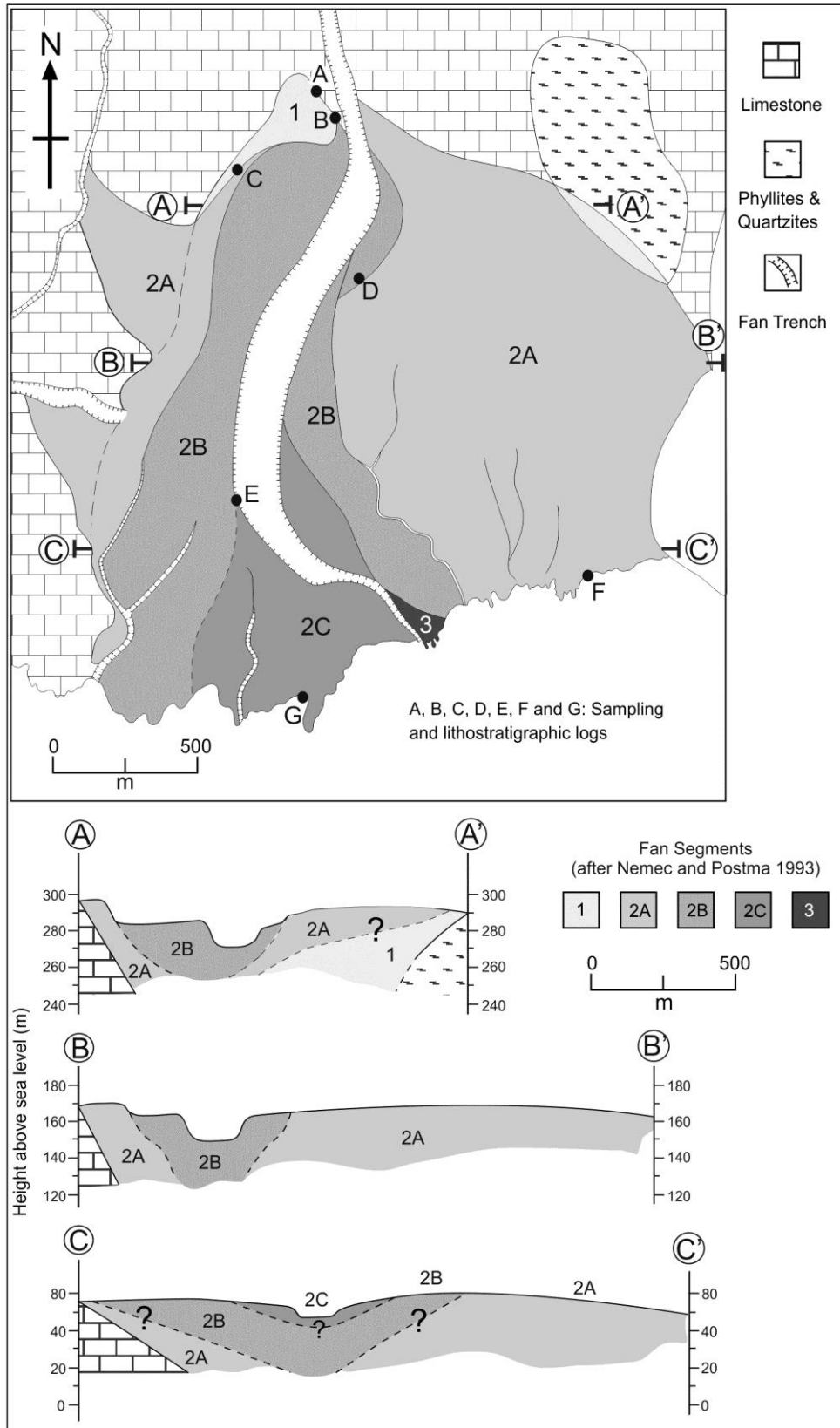


692

693 Figure 1 - The coastal piedmont and distribution of the Sphakia fan systems, southwest Crete. Note  
694 that Sphakia fan is indicated by the grey shading. Inset (A) shows the location of Tenaghi Philipon  
695 indicated by the letter A. Inset (B) shows the location of core site M40/71 indicated by the letter B in  
696 respect of the study area.

697

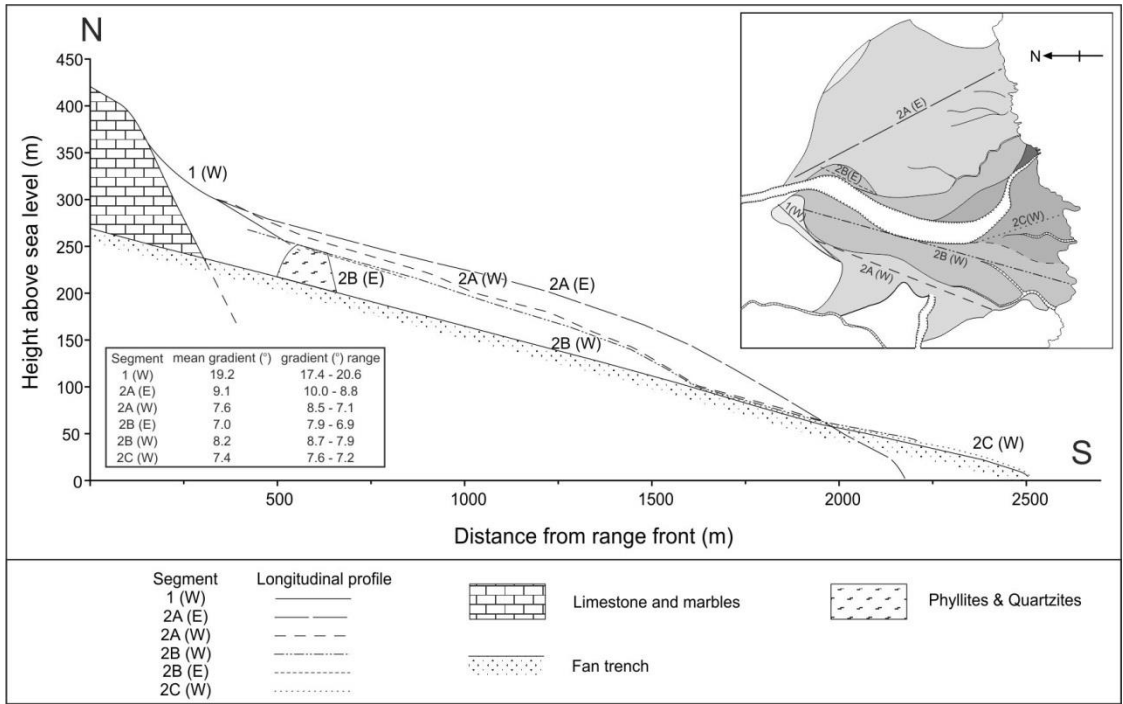
698 Figure



2

699 Simplified surface morphology and depositional stages within Sphakia fan (modified after Pope et  
 700 al., 2008). See text for a full discussion of the main depositional stages. Note that the letters A to G  
 701 refer to the OSL/U-series sampling locations and chronostratigraphies shown in Figure 5

702



703

704 Figure 3 Long profile of Sphakia fan. The inset indicates the locations of survey transects across  
 705 individual fan segments.

706

707

708

709

710

711

712

713

714

715

716

717

718

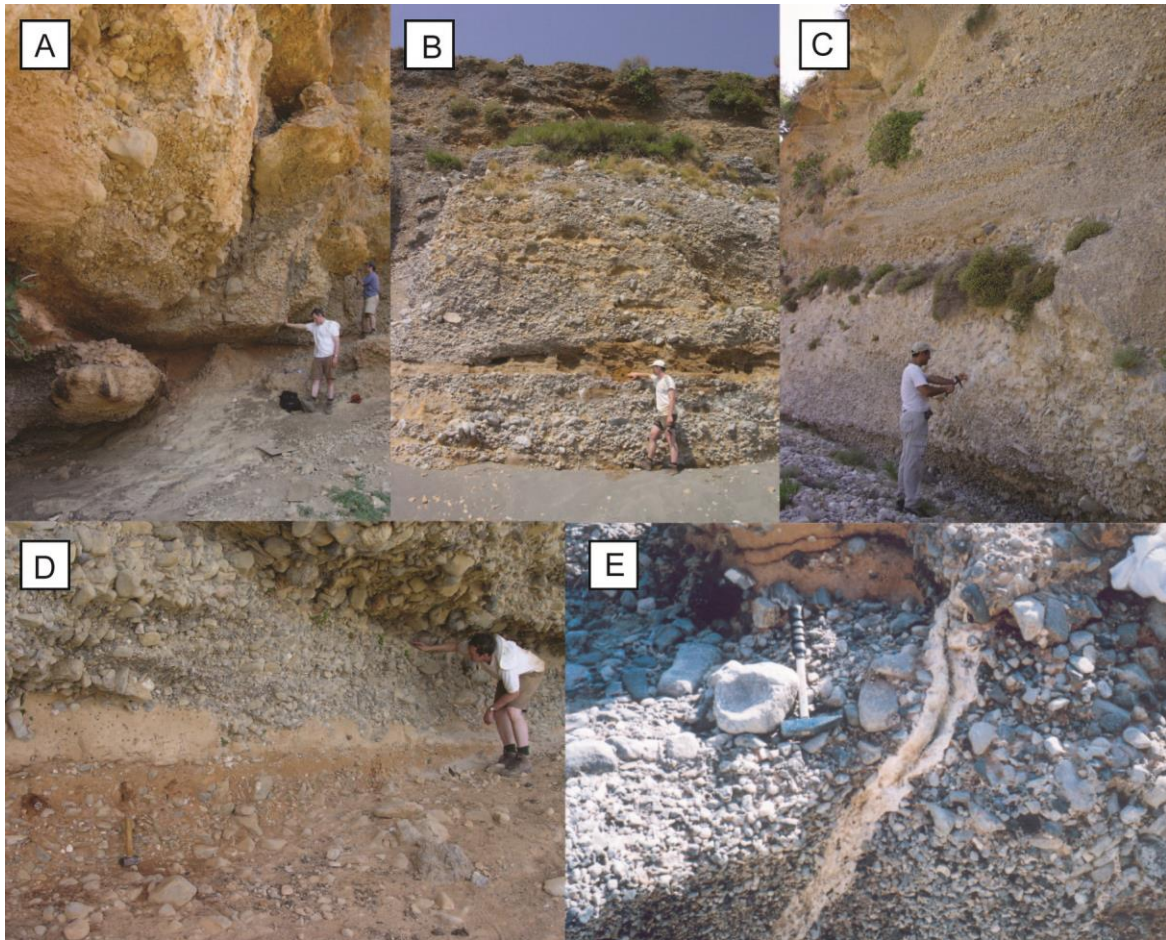
719

720

721

722

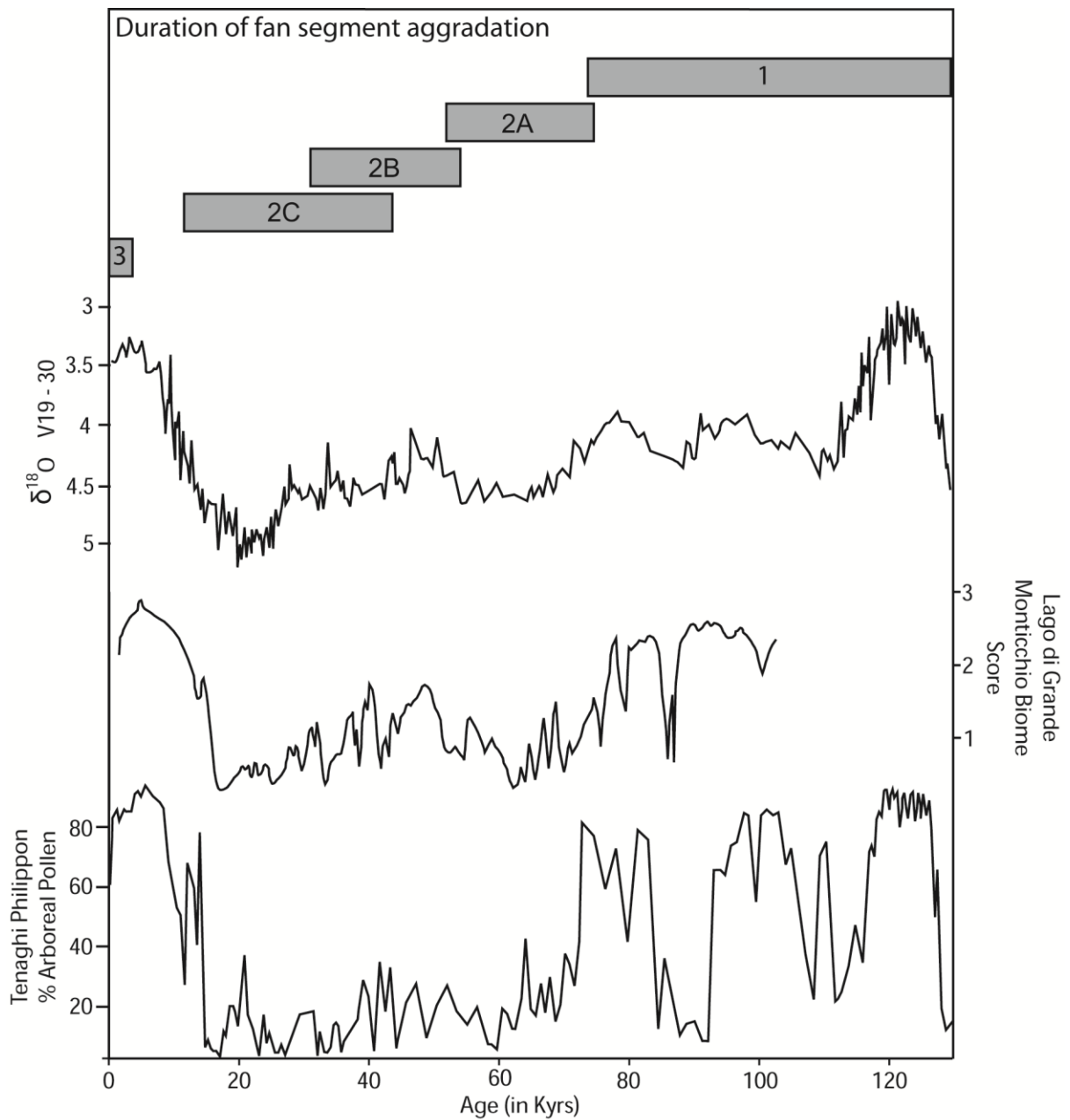
723



724

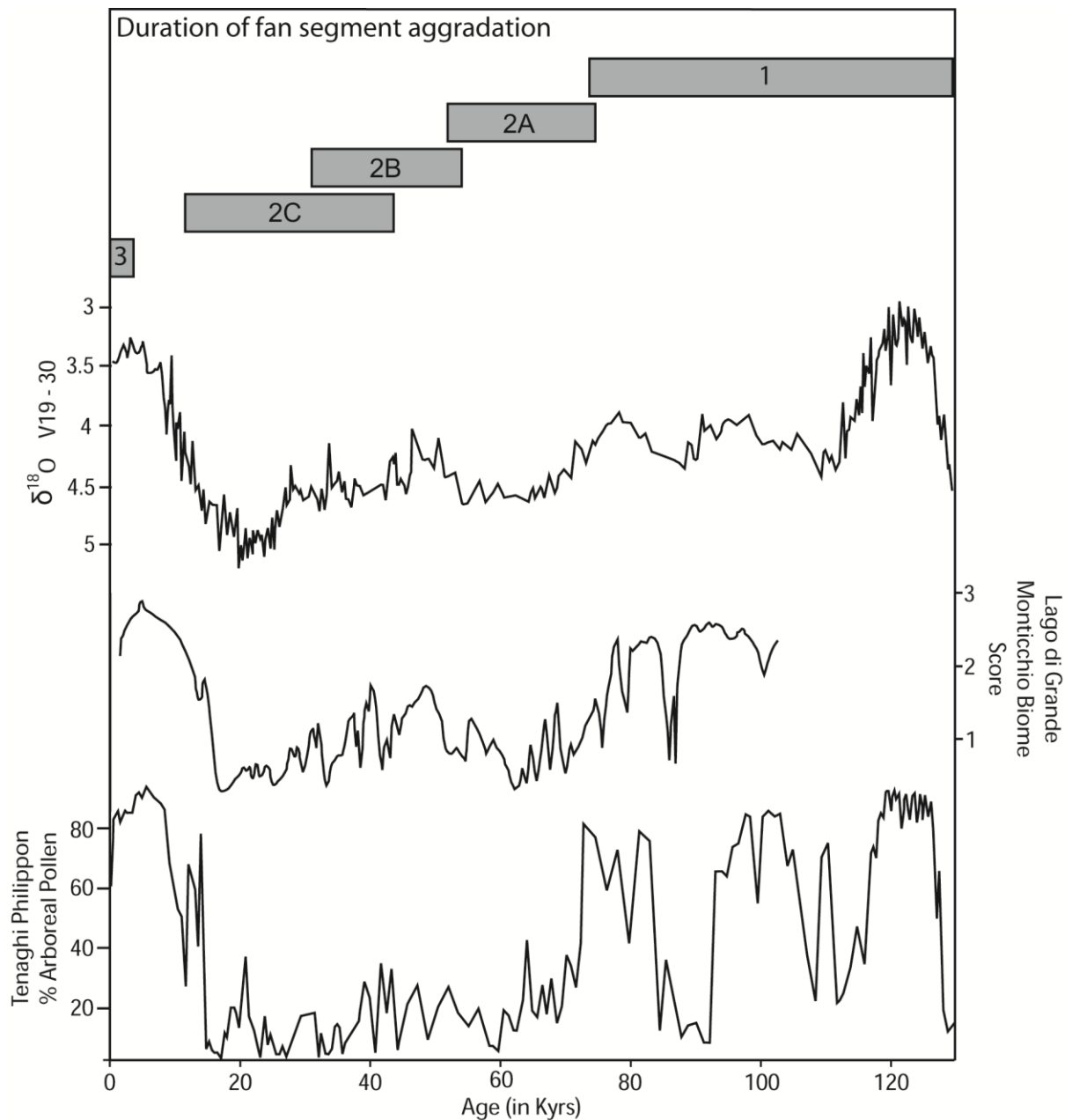
725 Figure 4 – Photographs showing the sedimentary characteristics of the deposits studied and dated in  
 726 this study. A) Segment 1 gravels showing poorly sorted characteristics typical of mass flow/debris  
 727 flow deposition. OSL dating of these sediments is based on the analysis of the fine-grained red units  
 728 that interbed with the coarser units (base of section) and the analysis of the inter-clast matrix. B)  
 729 Segment 2B gravels that express moderate sorting and crude horizontal stratification. The gravels  
 730 lenses are interbedded by the buff, fine-grained sediments that were the focus of OSL dating. C)  
 731 Segment 2B gravels showing well-developed horizontal stratification and a stronger degree of sorting.  
 732 D) Segment 2C gravels showing reddened fine-grained material interbedded with imbricated,  
 733 stratified gravels. E) A well-developed calcitic groundwater that has formed within the fan gravels.  
 734 The calcite has formed as a result of precipitation along a fault within the sediments. Cements also  
 735 develop as inter-clast, pore infill cements.





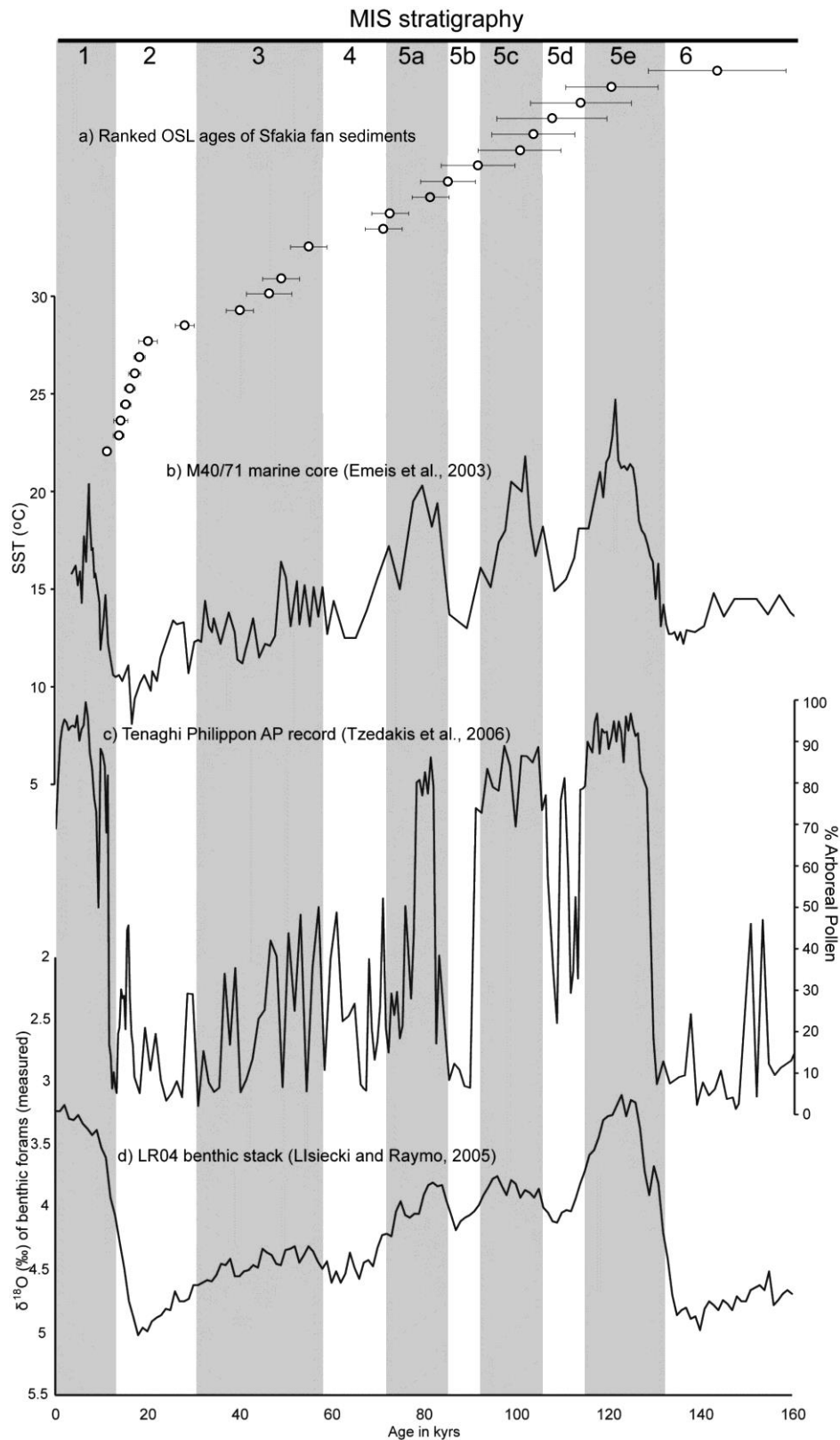
736

737 Figure 5 – OSL and U-series age estimates plotted against the stratigraphic logs of each sampling site.  
 738 See Figure 2 for the location of each site and Tables 1 and 2 for the data on which age estimate is  
 739 based.



740

741 Figure 6 – Age of fan depositional segments plotted against: (A) V19-30 benthic  $\delta^{18}\text{O}$  isotope record  
 742 (Shackleton et al., 1983); (B) Grande Lago di Monticchio Biome score (based on pollen assemblage  
 743 zones [Allen et al., 1999]); and (C) Tenaghi Philippon record of % arboreal pollen (excluding pine  
 744 (Tzedakis et al., 2006)).



745

746 Figure 7 – Age ranked OSL dates plotted against: (A) marine isotope stages; (B) sea surface  
 747 temperature data from southwest of Crete (Emeis et al., 2003); (C) the arboreal pollen record from  
 748 Tenaghi Philippon (Tzedakis et al., 2006); and (D) the LRO4 benthic stack (Lisiecki and Raymo,  
 749 2005).

750 Table 1. OSL determinations for the 180–250  $\mu\text{m}$  quartz fraction from the Sfakia fan

Risø code	Site	Depositional segment	Depth from surface (m)	$D_e$ (Gy/ka)	Aliquot No	$D_e$ (Gy)	Water content %*	Age (ka)
082401	Sfakia	1	15.2	$0.62 \pm 0.05$	23	$73 \pm 4$	24	$118 \pm 8$
062402	Sfakia	1	11.7	$1.49 \pm 0.08$	22	$137 \pm 6$	15	$92 \pm 6$
102404	Sfakia	1	7.5	$1.49 \pm 0.04$	23	$126 \pm 5$	12	$84 \pm 8$
102405	Sfakia	1	1.3	$1.14 \pm 0.03$	24	$82 \pm 2$	28	$72 \pm 3$
082402	Sfakia	1	14.8	$0.61 \pm 0.04$	32	$73 \pm 3$	12	$120 \pm 10$
082405	Sfakia	1	13.2	$0.74 \pm 0.05$	18	$81 \pm 3$	17	$110 \pm 9$
072404	Sfakia	1	11.9	$0.84 \pm 0.05$	16	$85 \pm 6$	31	$101 \pm 8$
102403	Sfakia	1	6.4	$1.49 \pm 0.04$	22	$121 \pm 5$	11	$81 \pm 4$
042412	Sfakia	1	5.8	$1.68 \pm 0.14$	26	$242 \pm 14$	26	$144 \pm 15$
072408	Sfakia	2B	3.8	$2.59 \pm 0.12$	17	$142 \pm 8$	9	$55 \pm 4$
042407	Sfakia	2B	21.3	$2.90 \pm 0.14$	24	$144 \pm 8.0$	5	$49 \pm 4$
062401	Sfakia	2B	1.0	$2.31 \pm 0.11$	27	$64 \pm 7$	27	$28 \pm 2$
082411	Sfakia	2C	16.2	$0.84 \pm 0.05$	18	$85 \pm 6$	31	$102 \pm 10$
082403	Sfakia	2C	14.5	$1.1 \pm 0.061$	22	$78 \pm 2$	8	$71 \pm 4$
042410	Sfakia	2C	8.9	$1.61 \pm 0.06$	30	$74 \pm 7$	22	$46 \pm 5$
072403	Sfakia	2C	19.8	$1.22 \pm 0.05$	25	$50 \pm 3$	40	$40 \pm 3$
072409	Sfakia	2C	7.6	$2.77 \pm 0.15$	27	$55 \pm 4$	7	$20 \pm 2$
062408	Sfakia	2C	3.3	$2.89 \pm 0.15$	25	$41 \pm 4$	9	$14.2 \pm 1.5$
062410	Sfakia	2C	0.9	$0.74 \pm 0.09$	13	$8.3 \pm 1.3$	18	$11.2 \pm 0.7$
072410	Sfakia	2C	3.5	$1.27 \pm 0.07$	17	$23.2 \pm 1.6$	2	$18.2 \pm 1.2$
072411	Sfakia	2C	2.9	$2.46 \pm 0.12$	22	$42.0 \pm 2.0$	2	$17.2 \pm 1.2$
072412	Sfakia	2C	2.3	$0.79 \pm 0.05$	20	$12.9 \pm 0.8$	2	$16.1 \pm 1.1$
072409	Sfakia	2C	1.9	$2.33 \pm 0.12$	18	$35.4 \pm 1.6$	2	$15.2 \pm 1.1$
062409	Sfakia	2C	0.9	$0.71 \pm 0.09$	13	$9.7 \pm 1.8$	18	$13.8 \pm 1.2$

751 The moisture content of the samples varied overtime in response to surface and groundwater fluctuations resulting from changes in humidity and base level. To ensure that  
752 realistic water content figures were calculated an average of the present-day and saturated water content values were derived for each sample since this represents the closest  
753 approximation of water content throughout the burial history (A. Murray, pers.comm.). Note that age estimates for 082401, 102404, and 082403 differ slightly to those  
754 presented in Ferrier and Pope (2012) due to a recalculation of the original sampling depths.

755 Table 2. U-series age estimates and geochemistry. All ages calculated using ISOPLOT (Ludwig, 2003)

Royal Holloway code	Sample description	$^{230}\text{Th} / ^{232}\text{U}$	Depositional segment	$^{230}\text{Th} / ^{238}\text{U}$	$^{234}\text{U} / ^{238}\text{U}$	Age ka
Cr-0615	Sparry cement* <sup>1</sup>	$5.18 \pm 0.14$	1	$0.74 \pm 0.02$	$1.08 \pm 0.0100$	$123.9 \pm 7.4$
Cr-0648	Sparry cement	$35.56 \pm 0.24$	1	$0.56 \pm 0.01$	$1.10 \pm 0.0049$	$75.4 \pm 2.9$
Cr-0617	Sparry cement	$34.42 \pm 0.25$	1	$0.55 \pm 0.01$	$1.13 \pm 0.0049$	$70.9 \pm 1.0$
Cr-0621	Sparry cement* <sup>2</sup>	$6.83 \pm 0.16$	2C	$0.74 \pm 0.02$	$1.09 \pm 0.0060$	$72.3 \pm 6.1$
Cr-0619	Soil carbonate* <sup>3</sup>	$1.81 \pm 0.03$	2C	$0.46 \pm 0.01$	$1.08 \pm 0.0100$	$59.0 \pm 2.3$
Cr-0616	Reworked Flow stone	$418.75 \pm 2.43$	2C	$1.04 \pm 0.01$	$1.02 \pm 0.0039$	>350
Cr-0639	Sparry cement	$19.01 \pm 0.14$	2C	$1.01 \pm 0.01$	$1.06 \pm 0.0100$	$300 \pm 21.0$
Cr-0650	Sparry cement	$298.32 \pm 2.34$	2C	$0.89 \pm 0.01$	$1.10 \pm 0.0043$	$172.8 \pm 4.3$

756 1,2, 3 - Detrital correction applied due to contamination, ages shown are corrected following Clark-Balzan et al. (2013)